Applied Catalysis B: Environmental 165 (2015) 10–19

Contents lists available at ScienceDirect

Applied Catalysis B: Environmental

journal homepage: www.elsevier.com/locate/apcatb

Ammonia formation over supported platinum and palladium catalysts

Emma Catherine Adams[a,*], Magnus Skoglundh[a], Milica Folic[b], Eva Charlotte Bendixen[b], Pär Gabrielsson[b], Per-Anders Carlsson[a]

[a] Competence Centre for Catalysis, Chalmers University of Technology, SE-412 96 Göteborg, Sweden
[b] Haldor Topsøe A/S, P.O. Box 213, DK-2800 Lyngby, Denmark

ARTICLE INFO

Article history:
Received 16 July 2014
Received in revised form
23 September 2014
Accepted 25 September 2014
Available online 6 October 2014

Keywords:
Catalytic exhaust aftertreatment
Passive-SCR
NO_x reduction
In situ DRIFT spectroscopy
NH_3 formation

ABSTRACT

We report experimental results for the formation of ammonia from nitric oxide and hydrogen, and from nitric oxide, water and carbon monoxide over silica, alumina and titania supported platinum and palladium catalysts. Temperature programmed reaction experiments in gas flow reactor show a considerable formation of ammonia in the temperature range 200–450 °C, which is suppressed by the presence of excess oxygen. However, oxygen sweep experiments show that for the titania supported catalysts minor amounts of oxygen promotes the ammonia formation at low temperatures. *In situ* DRIFT spectroscopy measurements indicate that cyanate species on the support play an important role in the ammonia formation mechanism. This work shows that alumina supported palladium is a promising system for passive selective catalytic reduction applications, exhibiting low-temperature activity during the water–gas-shift assisted ammonia formation reaction. Conversely, titania supported samples are less active for ammonia formation as a result of the poor thermal stability of the titania support.

1. Introduction

Combustion of petrol and diesel in vehicles results in the formation of harmful products, including nitrogen oxides (NO_x), which are known to be responsible for various environmental issues such as photochemical smog and acid rain [1,2]. At present, the fuel economy of passenger cars can be improved by ensuring that the combustion takes place in the presence of excess oxygen, so-called lean operation [3]. Practically, lean operation makes it challenging to reduce NO_x to N_2 over the conventional three-way catalyst [4]. Thus it is necessary for new strategies to be developed whereby the fuel economy can be improved whilst the tailpipe emissions are kept sufficiently low [5,6]. Selective catalytic reduction of NO_x with ammonia (NH_3-SCR) is currently the preferred technology for NO_x abatement from stationary sources and larger vehicles including trucks and buses [7]. Ammonia-SCR relies on the ability of the catalyst to selectively reduce NO_x with NH_3 to form N_2 in the presence of elevated levels of O_2 [8,2]. However, due to concerns with the safety and toxicity associated with ammonia transportation and storage, the NH_3 is stored in the form of urea-in-water solution on-board the vehicle. Urea solution is injected into the exhaust gas where it thermally decomposes and hydrolyses to form the ammonia required for NH_3-SCR [9,10]. Although this solution has been accepted for heavy-duty vehicles, difficulties arise when applied to smaller passenger vehicles. Some of the problems encountered are due to extra weight associated with the need for an additional urea storage tank and injection system, which is complex, costly and may affect driving performance negatively, and the risk of creating an NH_3 slip [2,4,11]. Ammonia emissions are undesirable since NH_3 is a toxic air pollutant and is known to contribute to the production of secondary particulate matter [12,13].

Passive SCR is a newly developing technology that may contribute to solving some of the aforementioned problems [14]. The concept of this technique is to generate NH_3 on-board the vehicle by utilizing the NO_x that is readily available in the exhaust stream whilst the engine undergoes rich operation (low air-to-fuel ratio). The formed NH_3 can then be stored on an SCR catalyst downstream and used to reduce slipped NO_x when the engine is set back to operate under lean conditions. If sufficient amounts of NH_3 can be produced during the rich periods and stored for complete reaction with NO_x to form N_2 during the subsequent lean periods, an external urea injection system may not be needed. It is well known that NH_3 can be formed over precious metal catalysts by the reaction between NO_x and H_2 provided that the stoichiometric requirement, i.e. $H_2/NO \geq 2.5$, is fulfilled. The overall reaction follows;

$$NO + \frac{5}{2} H_2 \rightarrow NH_3 + H_2O \quad (1)$$

* Corresponding author. Tel.: +46 31 772 29 07.
E-mail address: emma.adams@chalmers.se (E.C. Adams).

http://dx.doi.org/10.1016/j.apcatb.2014.09.064
0926-3373/

If the criterion on the H_2/NO ratio is not fulfilled, selectivity to other nitrogen-containing products has been observed [11,15,16], for example N_2O and N_2 by the two reactions:

$$NO + \frac{1}{2}H_2 \rightarrow \frac{1}{2}N_2O + \frac{1}{2}H_2O \quad (2)$$

$$NO + H_2 \rightarrow \frac{1}{2}N_2 + H_2O \quad (3)$$

In automotive applications deviations in driving patterns result in conditions where the concentration of H_2 present in the exhaust feed does not meet the requirement for ammonia formation for significant periods. Despite this, passive SCR may play an important role in NO_x abatement provided that a direct supply of H_2 is not necessary. Carbon monoxide and water are also present in the exhausts during rich operation [17] and H_2 can be formed by the water-gas-shift (WGS) reaction;

$$CO + H_2O \rightarrow CO_2 + H_2 \quad (4)$$

Hence, water could be a viable hydrogen source for the further formation of NH_3.

Previously Okumura et al. showed that SiO_2 and Al_2O_3 supported Pt and Pd catalysts have high selectivity to form NH_3 when in the presence of NO and H_2 at temperatures between 400 and 500 °C as compared to the corresponding Ir and Rh catalysts. In addition, Macleod et al. [2] showed that there is a synergy between Al_2O_3 and TiO_2 supports, which leads to further elevated formation of NH_3 in the presence of NO, CO and H_2O. This benefit can be ascribed to the hydrolysis of isocyanate groups, which is an additional well-documented route for NH_3 formation [15,18,17]. Although this process requires a catalytically active site (S) to form the initial surface isocyanate species (Eqs. (5) and (7)), the reaction steps responsible for the formation of NH_3 can take place both in the gas phase (Eq. (6)) and *via* an adsorbed species on the catalyst surface (Eq. (8));

$$S\text{-}NCO + H_2O \rightarrow S\text{-}OH + HNCO \quad (5)$$

$$HNCO + H_2O \rightarrow NH_3 + CO_2 \quad (6)$$

$$S\text{-}NCO + H_2O \rightarrow S\text{-}NH_2 + CO_2 \quad (7)$$

$$S\text{-}NH_2 + H_2O \rightarrow S\text{-}OH + NH_3 \quad (8)$$

The objective of the present study is to investigate whether or not NH_3 can be formed over a wide temperature window from NO + H_2 and NO + H_2O + CO gas mixtures over supported Pt and Pd catalysts, specifically addressing the role of the support material. This is carried out by a systematic comparison of silica, alumina and titania as support materials. Also, the influence of the presence of O_2 on the ammonia formation is studied.

2. Experimental

2.1. Catalyst preparation and characterisation

Supported Pt and Pd powder catalysts were prepared by incipient wetness impregnation of each of the following support materials: Al_2O_3 (Puralox SBa200), SiO_2 (Kromasil) and TiO_2 (Hombifine). The supports were thermally treated in air at 600 °C to remove impurities and stabilise the structure prior to impregnation. Thereafter, the saturation point of each support was determined and they were then suspended in the corresponding volume of aqueous solutions of either $(NH_3)_4Pt(NO_3)_2$ or $(NH_3)_4Pd(NO_3)_2$ to ensure all solution would be taken up by the support. All prepared catalysts were frozen in liquid N_2 and subsequently freeze-dried for approximately 12 h to ensure complete sublimation of water. The powder samples were then calcined at 550 °C in air for 1 h.

The powder catalysts were then coated onto cordierite monolith substrates. This was done by preparing solutions consisting of the powder catalyst, suitable binder materials based on support composition (Al_2O_3; Disperal P2, SiO_2; Colloidal SiO_2 and TiO_2; TiO_2 sol), water and ethanol. The monolith was then carefully immersed into the slurry, allowing the catalyst-containing liquid to be dispersed evenly throughout the channels by capillary forces. The monolith was then dried in air at 90 °C for two minutes to remove the water and ethanol, before being briefly calcined in air for a further two minutes at 500 °C and weighed. If necessary, the process was repeated until the desired mass of catalyst and binder was deposited (200 ± 3 mg). Once coated, the monoliths were calcined in air at 600 °C for 2 h to ensure complete removal of water. The specific surface area of the prepared samples was measured by nitrogen physisorption at −196 °C using an ASAP 2010 (Micrometrics) sorptometer. Prior to adsorption, all samples were dried at 200 °C for 2 h under vacuum in order to remove any residual water. Respective surface areas were then determined according to the standard Brunauer–Emmett–Teller (BET) method [19] using P/P_0 = 0.05–0.20. The specific surface area of the pure support materials; both fresh and after calcination in air at 600 °C for 1 h was measured to determine the thermal stability of the supports. The prepared powder catalysts were characterised directly after calcination.

Transmission electron microscopy (TEM) analysis was carried out to determine the average noble metal particle size for each catalyst. A small amount of sample was dispersed in ethanol in an ultrasonic bath for 20 seconds. One drop of the suspension was then placed onto a Cu-grid coated with lacey carbon. Between 6 and 14 images of each sample were recorded at different magnifications: 36 × 36–294 × 294 nm. Additionally, energy dispersive spectroscopy (EDS) analyses were acquired at each position investigated to locate and confirm the presence and type of metal particles.

Inductively coupled plasma optical emission spectroscopy (ICP-OES) analysis was used to confirm the noble metal content of all samples. A mass of 0.1–0.15 g of finely ground sample was digested in a solution containing HNO_3 and HCl at 200 °C for 20 min in a Milestone Ethos Plus microwave digestion unit. The resultant clear sample solution was then diluted using pure water (18.2 MΩ) and the metal content was quantified with an Agilent 720 ES ICP-OES instrument. Emission signals from the sample were compared to the signal from certified calibration standards containing 0–10 mg/l Pd or Pt.

To compliment the afore-mentioned characterisation techniques, powder X-ray diffraction (XRD) was also performed using a Bruker XRD D8 Advance instrument with monochromatic Cu$K\alpha_1$ radiation. The 2θ range of interest was 15°–85° and the step size and time employed were 0.041 and 1 s, respectively. The rotation speed of the sample during measurement was 60 rpm.

2.2. Kinetic measurements in gas flow reactor

Continuous gas flow reactor studies were carried out to determine the activity of the prepared catalysts. The reactor setup employed in this investigation has previously been described by Kannisto et al. [20]. The system consists of a quartz tube surrounded with a heating coil and insulation. It contains two thermocouples to measure the temperature 10 mm before and in the centre of the monolith sample. Two uncoated (blank) cordierite monoliths were placed on either side of the sample monolith in the quartz tube in order to reduce otherwise significant heat losses and achieve a nearly isothermal sample. The inlet gas composition was controlled using mass flow controllers (Bronkhorst Hi-Tech LOW-ΔP-FLOW) and the outlet gas composition was analysed using an FTIR gas-analyzer (MKS 2030 HS). All experiments were carried out

Table 1
Summary of gas compositions used in the temperature programmed reaction experiments.

	NO [ppm]	H_2 [ppm]	CO [ppm]	H_2O [%]
Feed 1	500	1500	–	–
Feed 2	500	–	1500	2
Feed 3	–	–	1500	2

with an Ar balance in order to keep the total gas flow constant at 2000 ml/min, corresponding to a space velocity of 40,000 h^{-1}.

Temperature programmed reaction experiments were carried out to investigate the temperature region for ammonia formation over the different samples. All samples were exposed to gas mixtures containing 500 ppm NO and either 1500 ppm H_2 (Feed 1) or 1500 ppm CO accompanied by 2 % H_2O (Feed 2), see Table 1. During exposure to both gas mixtures, the inlet temperature was varied from 500 to 120 °C at a rate of 6 °C/min. The system was then kept at this temperature for 10 min before increasing the temperature to 500 °C at the same rate. The low ramp rate was chosen as to ensure nearly stationary conditions. This scheme was carried out both in the absence and presence of 2% O_2. An additional experiment was carried out in order to determine the activity for the water–gas-shift reaction of the samples, represented by Feed 3 in Table 1.

Steady-state experiments at 250, 350 and 450 °C were carried out to evaluate the influence of the stoichiometric number, *S*, of the feed on the formation of NH_3 over the catalysts. The *S*-value characterizes the net oxidizing-reducing character of the inlet feed and is defined as [21];

$$S = \frac{2[O_2] + [NO]}{[CO] + [H_2]} \quad (9)$$

Again, the two feed compositions were fed to the reactor though this time various levels of oxygen were also added. The O_2 concentration was varied from 0.105 to 0.015% (corresponding to *S*-values between 1.73 and 0.33) in steps of 150 ppm, each of which lasted 20 min in order to allow steady state to be reached.

2.3. In situ infrared Fourier transform spectroscopy

Infrared Fourier transform spectroscopy was carried out *in situ* in diffuse reflection mode (DRIFTS) to follow the evolution of surface species during NH_3 formation. A Biorad FTS6000 spectrometer equipped with an *in situ* Harrick Praying Mantis reaction cell mounted with KBr windows was used. All samples were pretreated in an Ar flow at 450 °C for 30 min, cooled to 350 °C and a background spectrum was collected. The feed gas was then 500 ppm NO, 1500 ppm CO and 2% H_2O with varying concentration of O_2 ranging from 900 to 0 ppm (corresponding to *S*-values between 1.53 and 0.33) in steps of 150 ppm. Infrared spectra were recorded between 1200 and 3800 cm^{-1} after the catalyst had been exposed to each gas composition for 20 min. The spectra displayed in the figures are difference spectra, *i.e.*, the spectra obtained after background subtraction, in order to more clearly show the adsorbates as a function of the gas phase composition.

3. Results

3.1. Catalyst characterization

The catalysts prepared were characterised with respect to specific surface area, noble metal content and noble metal particle size. These results, together with the results for the specific surface area measurements of the pure support materials are summarised in Table 2. It can be seen that the surface area of the Al_2O_3 and SiO_2 supported catalysts remain relatively unchanged after both thermal treatment and noble metal impregnation. However, a large loss in surface area can be observed for the TiO_2 support when calcined at 600 °C. The metal content of all Pt containing catalysts was confirmed by ICP-OES analysis to be 1 wt.% ± 0.07 and that of the Pd series to be 0.5 wt.% ± 0.13.

In Fig. 1, the results from the XRD and TEM analysis of all samples are shown. The X-ray diffractograms of the pure support materials are also displayed as a reference in order to determine whether impregnation of the noble metal results in well-dispersed or larger particles. The diffractogram for the fresh TiO_2 support is also included in the analysis as a phase-change from anatase to rutile is suspected to be the explanation for the large decrease in surface area as a result of thermal treatment, as revealed by the BET analysis. However, XRD confirms that TiO_2 remains present in the form of anatase but the primary particles of the porous titania support have grown considerably after calcination at 600 °C. This can be concluded from the substantial increase in intensity of the diffraction peaks. In the case of the Pd impregnated samples, there appears to be no difference between the diffractograms of the impregnated sample and respective support material. This indicates that the Pd particles are either very small and well dispersed or too amorphous to be detected by XRD. However, a combination of both of these effects could also explain the absence of diffraction peaks related to Pd and should not be ruled out. X-ray diffraction peaks from metallic Pt (1 1 1) are detected for all supports impregnated with Pt and can be seen at 2θ = 40 ° (indicated in the diffractograms by the dashed line) [22]. The metal particle size range is determined using TEM imaging. The silica supported noble metal particles are easily detected during the analysis due to good contrast between the noble metal and the support. A

Table 2
BET, ICP-OES and TEM characterization of prepared samples.

Sample	Surface area [m^2/g]	Metal content [wt.%]	Noble metal particle size range [nm]
Fresh TiO_2	337	–	–
Calcined[a] TiO_2	42	–	–
Pd/TiO_2	41	0.37	[b]
Pt/TiO_2	39	0.97	[b]
Fresh SiO_2	322	–	–
Calcined[a] SiO_2	326	–	–
Pd/SiO_2	329	0.47	1.5–7
Pt/SiO_2	320	0.99	1–120
Fresh Al_2O_3	200	–	–
Calcined[a] Al_2O_3	201	–	–
Pd/Al_2O_3	192	0.49	[b]
Pt/Al_2O_3	188	0.93	2–21

[a] After calcination in air at 600 °C for 1 h.
[b] Samples in which the location of metal particles is unclear.

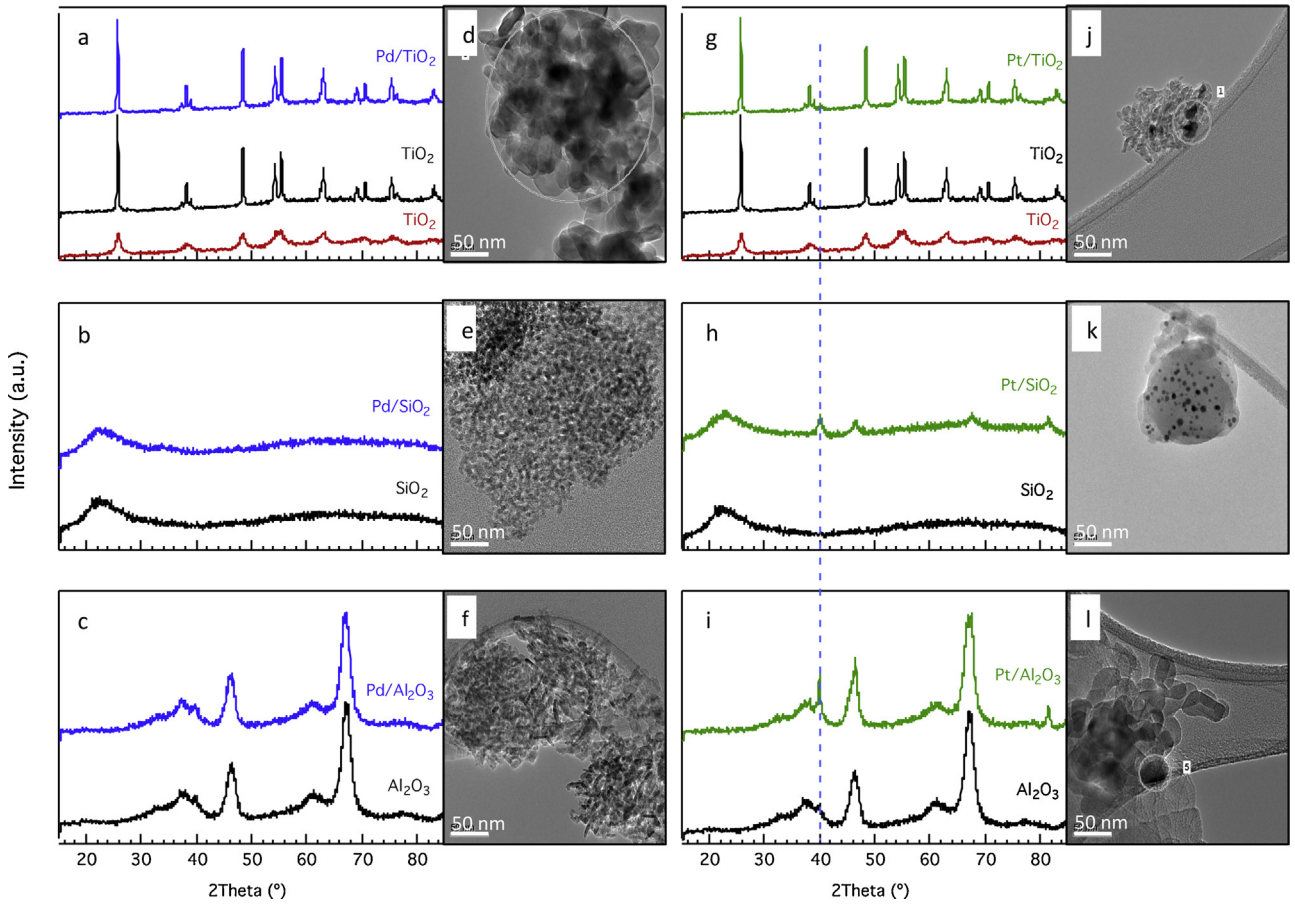

Fig. 1. XRD diffractograms of (a) Pd/TiO_2, (b) Pd/SiO_2, (c) Pd/Al_2O_3, (g) Pt/TiO_2, (h) Pt/SiO_2 and (i) Pt/Al_2O_3. Diffractograms of the pure supports are also included for reference. TEM images of (d) Pd/TiO_2, (e) Pd/SiO_2, (f) Pd/Al_2O_3, (j) Pt/TiO_2, (k) Pt/SiO_2 and (l) Pt/Al_2O_3. The dashed line indicates the position of diffraction from Pt(1 1 1). The scale bars measure 50 nm.

relatively narrow range of small particles was observed for the Pd sample (1.5–7 nm) whereas a much wider range is observed for the silica support impregnated with Pt (1–120 nm). It was also possible to measure noble metal particle size for the Pt/Al_2O_3 sample. Comparing Pt/SiO_2 with Pt/Al_2O_3, we see a much broader range in size of noble metal particles on the SiO_2 supported sample than that of the Al_2O_3 supported sample (2–21 nm). From the TEM micrographs for Pd/TiO_2, Pt/TiO_2 and Pd/Al_2O_3, it is difficult to distinguish individual metal particles (represented in the table by [b]). In the case of Al_2O_3 and TiO_2 supported Pd, although the particles could not be distinguished well enough to determine their size, their presence was confirmed by EDS.

3.2. Kinetic measurements in gas flow reactor

Fig. 2 shows the formation of NH_3 over the catalysts in the presence of NO and H_2 (Feed 1) as a function of the inlet gas temperature. The inlet concentration of NO is 500 ppm, thus the maximum concentration of NH_3 that can be achieved at steady-state is 500 ppm. It can thus be seen that near complete conversion of NO to NH_3 takes place over the SiO_2 and Al_2O_3 supported catalysts between 300 and 425 °C. Below 200 °C, the catalysts containing Pt show higher activity for NH_3 formation than their Pd containing counterparts. When exposed at these low temperatures formation of N_2O and N_2, although in low quantities, is observed over all samples. At high temperature, >400 °C, the type of support appears to have the dominating effect on the formation of NH_3. Neither of the TiO_2 supported catalysts achieve considerable conversion of NO to NH_3 when compared to the corresponding SiO_2 and Al_2O_3 supported samples. The maximum conversion to NH_3 observed over the titania supported samples is around 50 and 60% for the Pd and Pt containing catalysts, respectively. When repeated in the presence of excess O_2, the formation of N_2O and NO_2 is detected although most of the NO remains unreacted. In general, more NO_2 is formed over Pt-containing samples over a broader temperature range, with a maximum of ca. 150 ppm observed over Pt/SiO_2 centered at a temperature of 300 °C, compared to ca. 50 ppm formed over Pd/SiO_2 at 420 °C. Small amounts of N_2O are again observed at temperatures below 200 °C. The Pt-containing samples were again found to be more active for the formation of this undesirable product, with an average production of 100 ppm N_2O compared to ca. 20 ppm over the Pd-containing catalysts.

Fig. 3a and b shows the formation of NH_3 and CO_2 in the presence of NO, CO and H_2O (Feed 2) as a function of inlet gas temperature for all catalysts whilst Fig. 3c shows the corresponding CO_2 production in the presence of CO and H_2O only (Feed 3). At temperatures below 275 °C, the formation of H_2 is higher over all Pd containing samples as compared to those catalysts that contain Pt. However, this trend reverses above this temperature when, with the exception of Pd/Al_2O_3, the hydrogen formation over the Pt containing samples is higher than over the corresponding Pd catalysts. This corresponds well with the results in Fig. 3a which show that the formation of NH_3 generally is higher over the Pd samples below 275 °C and over the Pt samples when this temperature is exceeded. However, this effect cannot only be explained by the WGS activity of the catalysts, since more NH_3 is seen to be formed between 200 and 400 °C in Fig. 3a than H_2 is formed in Fig. 3c during the pure WGS reaction (absence of NO). In fact, the increased CO_2 formation

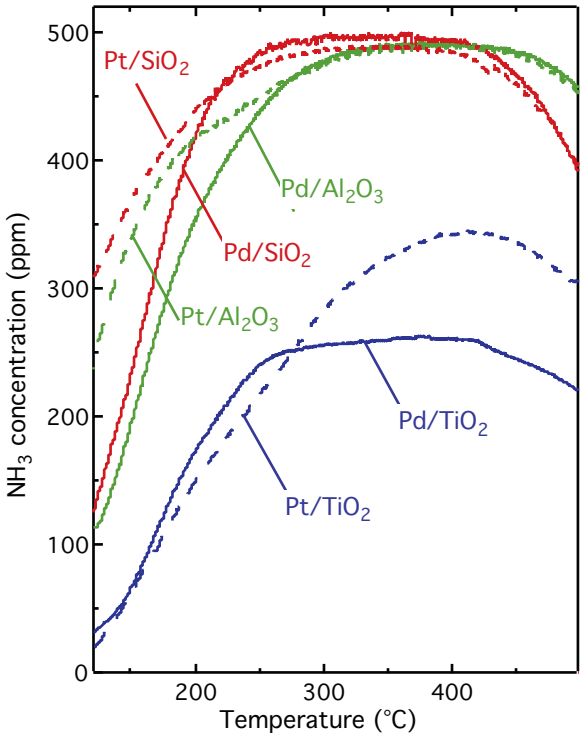

Fig. 2. Ammonia formation over silica, alumina and titania supported Pt and Pd catalysts during temperature programmed reaction using 500 ppm NO and 1500 ppm H_2 in Ar in the gas feed and a temperature ramp rate of 6°C/min. The space velocity was 40,000 h^{-1}.

observed in Fig. 3b may explain this behaviour and is discussed further in the final section. Unlike in the previous experiment with H_2 and NO (Feed 1), the Al_2O_3 supported catalysts are now found to be more active than their SiO_2 supported counterparts. Interestingly, during the WGS-assisted experiments, the TiO_2 supported catalysts do not appear as inferior for NH_3 formation as they do when H_2 is available directly in the feed gas. In fact, both samples are able to form higher amounts of NH_3 than the Pd/SiO_2 catalyst. With regards to N_2O, it is observed that this product is now formed over a much broader temperature range (200–400 °C) than when H_2 was directly available in the gas feed. On average, 40 ppm N_2O is produced over the Pd-containing samples whilst around 10 ppm is detected over their Pt-containing counterparts. Unlike the case when H_2 is directly available in the gas feed, no N_2 is formed at low temperatures when water is used as the source of hydrogen. However, N_2 starts to form at temperatures exceeding about 350 °C. When this experiment is repeated in the presence of excess O_2, NO_2 is formed in very similar amounts to those described for the same reaction with H_2 directly available in the feed. As before, most of the NO remains unreacted in the presence of excess O_2. However, no N_2O is formed over any sample when using CO and H_2O as reductants.

Fig. 4 shows the steady-state formation of NH_3 from NO and H_2 over the catalysts as a function of the stoichiometric number of the feed at 250, 350 and 450 °C. The stoichiometric number is varied by varying the oxygen concentration of the feed, where $S < 1$ represents a net-reducing feed and $S > 1$ is net-oxidizing. When the concentration of oxygen fed to the reactor is 500 ppm the feed is stoichiometrically balanced and the S-value is 1.0. For all samples, it can be seen that the NH_3 formation starts when the S-value is lower than 1.0 and increases significantly upon decreasing S-value. With the exception of Pt/TiO_2, altering of the inlet gas temperature has negligible effect on the NH_3 formation over the samples when hydrogen is included in the feed gas.

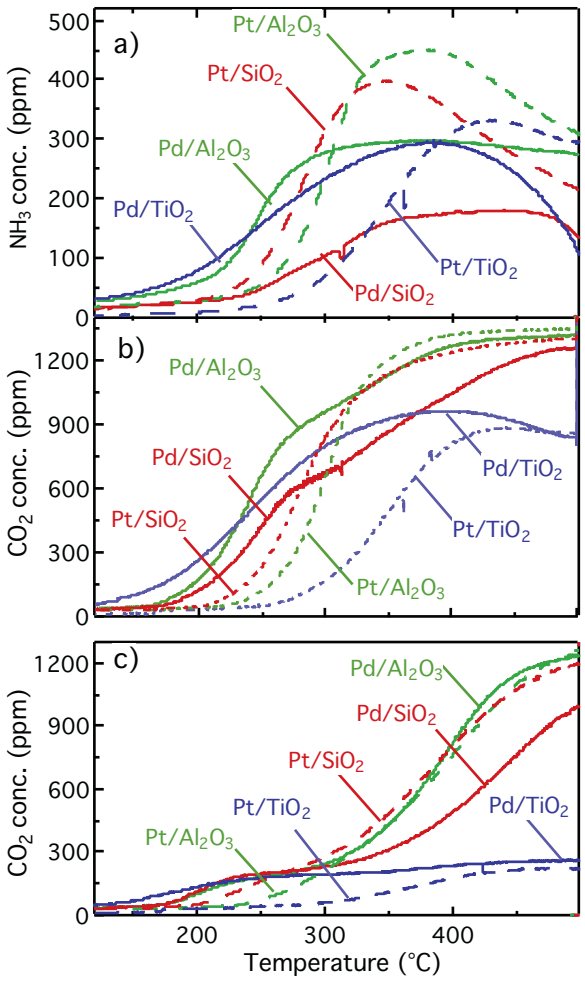

Fig. 3. Temperature programmed reaction experiments; formation of (a) ammonia (b) carbon dioxide during WGS-assisted formation of NH_3 using 500 ppm NO, 1500 ppm CO and 2% H_2O in Ar in the gas feed. Panel (c) shows the formation of carbon dioxide during WGS conditions feeding 1500 ppm CO and 2% H_2O in Ar. In all experiments a space velocity of 40,000 h^{-1} was used

The corresponding experiments for the influence of the S-value on the WGS-assisted NH_3 formation are displayed in Fig. 5. Again we see that the formation of NH_3 starts when the feed becomes net-reducing and increases significantly with decreasing S-value. However, in contrast to the corresponding experiment with H_2 and NO, the ammonia formation from the feed with H_2O, CO and NO is clearly dependent on the temperature. At 250 °C, NH_3 is exclusively formed over those catalysts which contain Pd with the exception of silica supported Pd. However, at higher temperatures, the NH_3 formation increases over the Pt containing catalysts. These results further correlate with the H_2 formation trends observed in Fig. 2b where it can be seen that the Pd samples are more active at low temperatures whereas the Pt samples are more active at higher temperatures. An interesting observation during both the hydrogen and the WGS oxygen dependence reactions over Pt/TiO_2 at elevated temperatures (350 and 450 °C), is that the presence of 150 ppm O_2 ($S = 0.53$) results in higher NH_3 formation than complete absence of O_2 in the feed.

3.3. *In situ* DRIFT spectroscopy

The results from the *in situ* DRIFT spectroscopy experiments for the alumina and titania supported platinum samples during WGS-assisted ammonia formation conditions as a function of the S-value

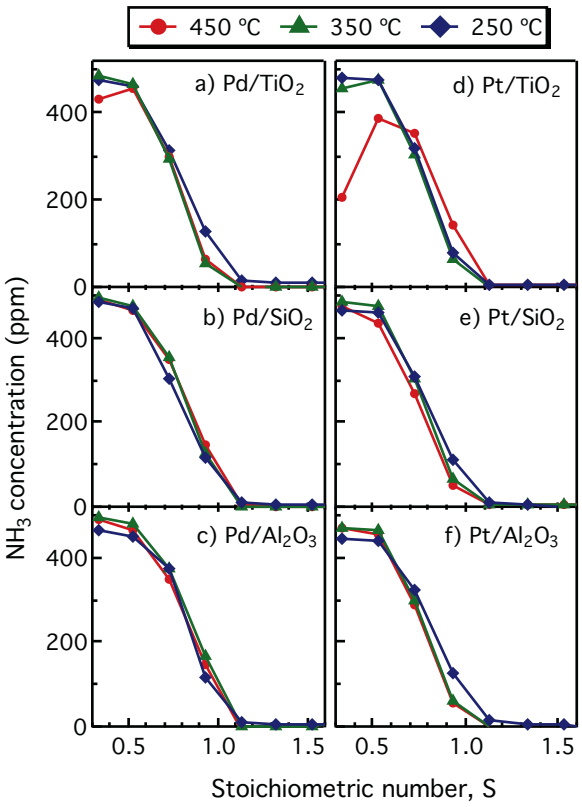

Fig. 4. Steady-state formation of NH_3 versus oxygen concentration at 250, 350 and 450 °C. The gas feed contained 500 ppm NO and 1500 ppm H_2 while the O_2 concentration was varied between 0 and 1050 ppm (S = 0.33–1.73) in steps of 150 ppm. Ar was used as balance and space velocity was 40,000 h^{-1}.

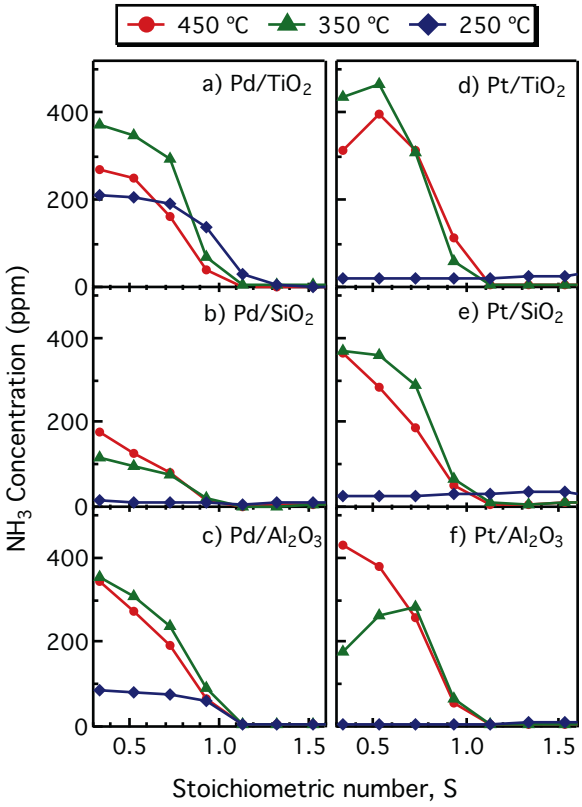

Fig. 5. Steady-state WGS assisted formation of NH_3 versus oxygen concentration at 250, 350 and 450 °C. The gas feed contained 500 ppm NO, 1500 ppm CO and 2% H_2O while the O_2 concentration was varied between 0 and 1050 ppm (S = 0.33–1.73) in steps of 150 ppm. Ar was used as balance and space velocity was 40 000 h^{-1}.

are shown in Fig. 6. The corresponding results for the alumina and titania supported Pd samples are shown in Fig. 7. The stoichiometric number of the feed employed during each step is displayed on each spectrum and those experiments carried out under net-oxidizing conditions are represented by blue spectra, whereas those performed in the presence of net-reducing feeds are represented by green spectra. All peak assignments made are summarised together with references to previous studies in Table 3.

In the presence of excess O_2 ($S > 1$) a significant absorption band representing gaseous CO_2 (2350–2360 cm^{-1}) can be observed for all samples. As the O_2 concentration is lowered, the contribution of this band decreases significantly. This is accompanied by an increased band intensity for both bridge-bonded (1936 cm^{-1}) and linearly adsorbed (2050 – 2070 and 2080 cm^{-1}) CO on Pt and Pd as well as an observed increase in the intensity of the NH stretching vibrations in the 3150 - 3400 cm^{-1} region, corresponding to an increase in the amount of surface bound NH_3. An increase in the intensity of bands due to the adsorption of NH_2 is also observed at 1321 cm^{-1} for both TiO_2 supported catalysts. For both Al_2O_3 supported catalysts, an absorption band representative of cyanate groups (2240 cm^{-1}) can be seen once the feed becomes net-reducing. This band shows an initial increase when the S-value is decreased. However, after the S-value reaches 0.73, the intensity of this band starts to decrease, having negligible contribution to the spectra obtained in the absence of oxygen. Again, this trend is accompanied by an increase in intensity of the absorption bands in the NH stretching region (3150–3400 cm^{-1}) showing an increase in surface bound NH_3. Also worth mentioning is the notable absence of peaks representative for noble metal coordinated NO (1668, 1746 and 1828 cm^{-1}) and support bound nitrates (1440,

Table 3
Summary of vibration and species assignments for the *in situ* DRIFTS experiments. (s) and (as) represent the symmetric and asymmetric stretching vibrations respectively.

Wavenumber (cm^{-1})	Vibration	Species	Ref.
1321	H—N—H (as)	NH_2 on TiO_2	[26]
1440	CO_2 (as)	Bicarbonate on Al_2O_3	[27,28]
1460	N=O (s)	Linearly bound nitrate on Al_2O_3	[28]
1590	N=O (s)	Chelating bidentate nitrate on Al_2O_3	[28]
1610	N=O (s)	Bridge-bonded bidentate nitrate on Al_2O_3	[28]
1668	N=O (s)	Linearly bound NO on Pt	[29]
1746	N=O (s)	Linearly bound NO on Pd^0	[30]
1828	N=O (s)	Linearly bound NO on Pd^+	[30]
1936	C=O (s)	Bridge-bonded CO on Pd	[31]
2050–2070	C=O (s)	Linearly bound CO on Pt	[32]
2080	C=O (s)	Linearly bound CO on Pd	[6,31]
2260	C=N (s)	Isocyanate (—CNO) on Al_2O_3	[6,33,31,34]
2350–2360	C=O (s)	Gaseous CO_2	[29,33,34]
3150–3400	N—H (s)(as)	NH_3 bound to Lewis acid sites	[2,35,36]

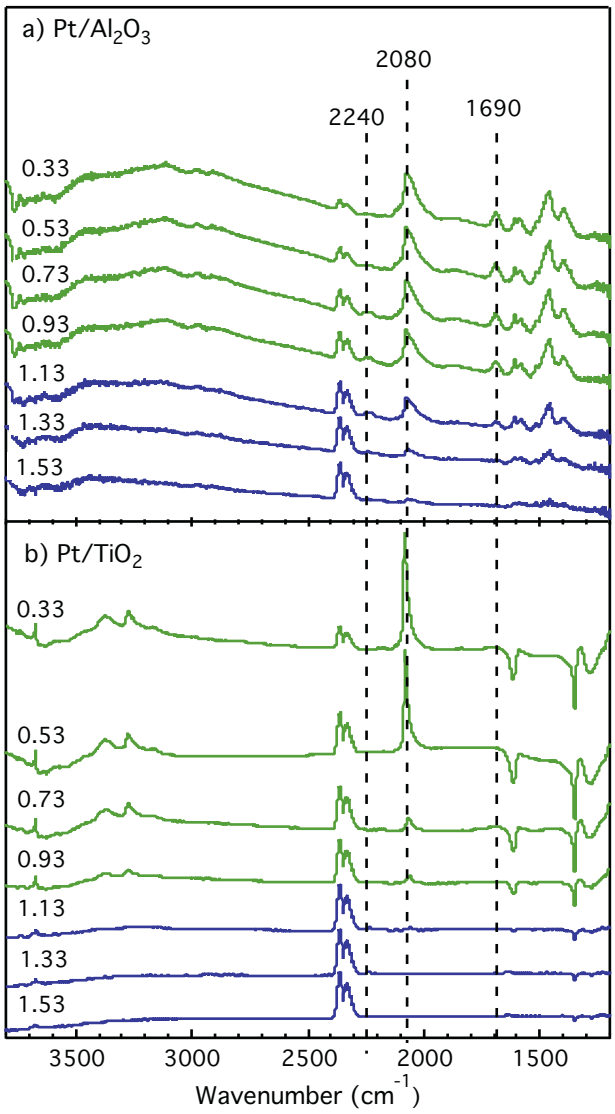

Fig. 6. DRIFT spectra acquired on a) Pt/Al_2O_3 and b) Pt/TiO_2 at constant temperature (350 °C) with inlet concentration of 500 ppm NO, 1500 ppm CO and 2% H_2O. O_2 concentration was varied between 0 and 1050 ppm (S = 0.33–1.53) and is represented by the stoichiometric value of the gas feed. Ar balance was employed during all steps.

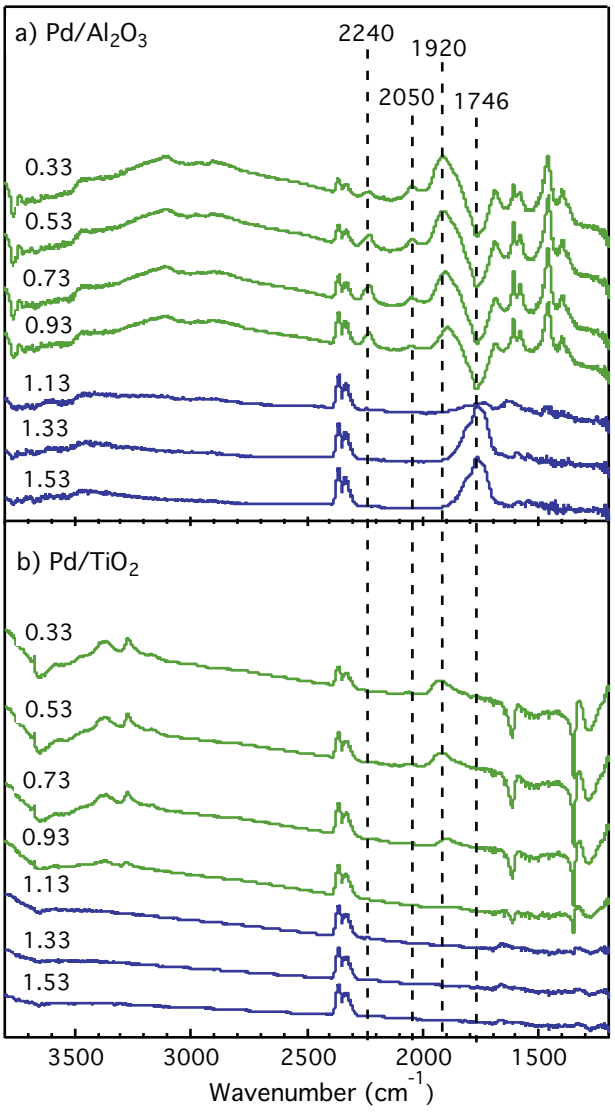

Fig. 7. DRIFT specta aquired on a) Pd/Al_2O_3 and b) Pd/TiO_2 at constant temperature (350 °C) with inlet concentration of 500 ppm NO, 1500 ppm CO and 2% H_2O. O_2 concentration was varied between 0 and 1050 ppm (S = 0.33–1.53) and Ar balance was employed

1460, 1590 and 1610 cm^{-1}) in the presence of excess oxygen for the Al_2O_3 supported samples. However, all these bands increase significantly and simultaneously as the feed becomes net-reducing.

For the Pd/Al_2O_3 sample, in the presence of excess O_2, an intense absorption peak ascribed to linearly adsorbed NO on Pd^0 (1746 cm^{-1}) can be observed. However, upon reducing the S-value of the feed below 1.0, this peak rapidly levels out before becoming negative. The evolution of the negative peak is accompanied by the detection of a small shoulder peak representative of linearly adsorbed NO on Pd^+ (1828 cm^{-1}), indicating the presence of two different Pd adsorption sites.

For the two titania supported samples, fewer and less intense absorption bands are observed during the *in situ* DRIFT experiments. For both samples, there is also a notable contribution of a sharp negative peak at 1610 cm^{-1}. Since the samples are pretreated with O_2 before a background spectrum is taken, it is assumed that the Pd and TiO_2 particles are in an oxidized state. Bickmore et al. have previously assigned an absorption band at 1610 cm^{-1} to physisorbed H-bonded water [23]. Furthermore, Benesi et al. [24] observed an absorption peak at 1610 cm^{-1} after exposing silica to H_2O. However, upon injection of D_2O in place of H_2O, the authors found that the position of this peak remained unchanged. As a result, the authors suggested that this band is due to surface silanol groups. In our case, it may not be unreasonable to suggest that we too observe surface hydroxyl groups at this position. It has previously been reported that OH groups on TiO_2 can readily combine to form Ti-O-Ti [25]. Thus, the increase in intensity of these negative peaks as the feed becomes increasingly net-reducing is suspected to be related to the reduction of surface hydroxyl groups on the titania supported sample. Hence the negative peaks observed in the DRIFTS-spectra.

4. Discussion

We have shown that by using NO and H_2, either direct or formed from water and CO *via* the water–gas-shift reaction, considerable amounts of ammonia can be formed over silica, alumina and titania supported platinum and palladium catalysts in a fairly broad temperature interval ranging from 200 to 450 °C. With the

assumption that no significant storage of NH_3 on the catalyst takes place, near complete conversion of NO to NH_3 over the Al_2O_3 and SiO_2 supported catalysts is possible when H_2 is directly available in the feed. The decrease in NH_3 formation above 425 °C, with no accompanying change in NO conversion, indicates that ammonia starts to decompose, forming elemental N_2 and H_2 at high temperatures [16,37]. We have also shown that oxygen is detrimental to the ammonia formation, however, in some cases a minor oxygen supply may be beneficial. The results that are obtained point towards a dependence on not only the support material of the catalyst but also the type of noble metal for adequate production of the desired NH_3. In the following we will discuss the roles of, on one hand, the noble metals and, on the other hand, the support materials for the ammonia formation mechanism.

To allow fair comparison of the influence of the noble metal (Pt or Pd) on the activity for ammonia formation, the molar amount of noble metal was kept constant during catalyst synthesis, *i.e.* the platinum catalysts were prepared with a noble metal loading of 1.0 wt.% whilst the palladium catalysts a loading of 0.5 wt.%. The results from the ICP-OES measurements confirm the targeted loadings. One should notice, however, that the same molar amount of noble metal is not the only criterion for a fair comparison as the precious metal dispersion and/or particle size distribution may be rather different between the different samples, which of course may influence the catalytic properties [22]. This is due to varying degree of interaction between the noble metal and metal oxide support, which is unique in each case. Generally silica is considered to interact more weakly with noble metals than alumina and titania [38]. From the TEM analysis this is recognized by relatively large noble metal particles for the silica samples. Unfortunately we could not make a proper particle size distribution analysis due to the inability to distinguish individual noble metal particles in Pd/Al_2O_3 and the titania supported samples. This is most likely due to small and/or oxidized metal particles resulting in too low contrast/resolution. Interestingly in the case of Pt/TiO_2, although the expected Pt content is confirmed *via* ICP-EOS analysis, platinum is neither observed by TEM nor EDS analysis. This may suggest that instead of well-dispersed Pt particles, the sample consists of larger particles not identified. This is supported by the presence of the sharp X-ray diffraction peak from metallic Pt (1 1 1), but is also confirmed by the *in situ* DRIFTS results showing a very sharp and intense absorption band for linearly adsorbed CO during oxygen-free conditions (*cf.* Fig. 6), which is expected for extended facets [39]. However, despite these differences between the samples it is still possible to compare the types of noble metals and support materials from the point of view of catalyst systems. Furthermore we mention that experiments (not shown) with significantly lower Pt loading gave nearly the same quantitative result, which supports that differences in noble metal dispersion of the present samples is not critical for the conclusions made here. Also, thanks to the *in situ* DRIFTS experiments the mechanism behind ammonia formation can be discussed in more detail.

The kinetic measurements in the flow reactor clearly show that the type of metal employed in the catalyst formulation has a significant effect on the NH_3 formation. At temperatures below 200 °C, when hydrogen is available in the feed, the Pt containing samples produce significantly more NH_3 than their Pd counterparts (*cf.* Fig. 2). On the contrary, below 250°C during WGS-assisted reaction conditions, the trend appears to switch so that the Pd containing samples show increased activity as compared to the Pt containing counterparts (*cf.* Fig. 3). This trend can also be seen in the steady-state experiments in Fig. 5, for which no NH_3 is formed over the Pt samples at 250 °C although the TiO_2 and Al_2O_3 supported Pd samples are active under these conditions. This can partly be explained by the enhanced low-temperature WGS activity over Pd compared to that of Pt, and has previously been reported in the literature [17]. It can also be seen that at higher temperature (300 °C) higher amounts of NH_3 are formed over the Pt samples. These results are in line with those of Cant et al. [40] who observed that NO removal over Pt/Al_2O_3 in the presence of H_2 and CO is only evident above 220 °C. The authors suggested that Pt and Pd surfaces are more prone to be covered by CO than NO and that this effect is more pronounced on Pt than Pd. Our *in situ* DRIFTS results support this suggestion as the build-up of linearly adsorbed CO as the *S*-value is lowered is more pronounced and occurs at higher *S*-values for the Pt samples than for the Pd samples. According to Cant et al. [40], this surface coverage is detrimental to NO_x reduction since the surface becomes predominantly covered by CO, which displaces NO and hinders the dissociative adsorption of H_2 required for the reduction of NO. Once hydrogen is dissociated, the H adatoms are considered to facilitate the reduction of NO by removal of O adatoms from dissociated NO or by hydrogen-assisted NO dissociation. Macleod et al. [41] also reported that the presence of CO has a negative effect on the reduction of NO on Pt, shifting the activity window for NO reduction towards higher temperatures. Moreover, they also showed that the presence of CO has a beneficial effect on the reduction of NO with H_2 over Pd systems. This can explain why reduced activity is observed over Pt-containing samples during the steady-state WGS assisted reactions at $S = 0.33$ as compared to when a slight O_2 availability is present ($S = 0.53$). The presence of metallic palladium, Pd^0, in excess oxygen is consistent with previously reported results by Miller et al. [30]. In their work the authors suggest that this site is responsible for the oxidation of CO to CO_2 and since the vibration from this species disappeared below the stoichiometric point for CO oxidation (shifting instead towards Pd^+), this suggestion seems reasonable.

Turning the focus on the role of the support material, it is clear that alumina and titania generate the most of the discussion in the present study and are probably the most interesting materials for future work. Also, as mentioned in the Introduction, Macleod et al. [2] proposed that Al_2O_3 enhances the hydrolysis of surface-bound cyanate (—NCO) groups to NH_3 whilst TiO_2 supports promote the formation of —NCO groups. Hence, we focused the *in situ* DRIFTS experiments on the WGS-assisted NH_3 formation over Al_2O_3 and TiO_2 supported catalysts, specifically addressing the influence of the stoichiometric number of the feed.

Since it is thought that one route for NH_3 formation proceeds *via* direct reaction of H_2 with adsorbed NO [11,15], the reduced NH_3 formation observed over the TiO_2 samples when H_2 is available in the feed during the temperature programmed reaction experiments may be related to the reduced surface area caused as a result of high-temperature treatment. It is possible that the loss of surface area of the support results in a lowered NO adsorption capacity thus resulting in less NO available to react with H_2. Upon observation of the DRIFT spectra obtained for both the TiO_2 samples, the intensity of the observed absorption bands for the Pd/TiO_2 sample is very low. Again, this is most likely related to the reduced surface area upon calcination, possibly suggesting that many of the active Pd particles present in the sample have been engulfed by the support during the growth of TiO_2 particles. This makes the active sites increasingly difficult to reach, reducing the adsorption capacity for reactant molecules. Another feature of the DRIFT spectra, which supports the explanation that it is the limited adsorption capacity of this sample which negatively affects its activity, is the absence of absorption bands representative of cyanate groups. Since Macleod et al. [2] propose that TiO_2 promotes the formation of cyanate groups on its surface, we would have expected to see a more substantial contribution of these peaks to the obtained spectra than those on the Al_2O_3 support. However, no such peaks were observed at all, indicating a significant loss of active sites on the sample. From the results in this study, it can be concluded with some confidence that there is more than one route possible for NH_3 formation using

NO, CO and H_2O as reactants since NH_3 was detected over the TiO_2 supported samples despite the absence of cyanate groups.

An interesting trend observed for the TiO_2 supported samples is the enhanced activity for NH_3 formation when in the presence of some O_2 ($S = 0.53$) as compared to total absence of oxygen ($S = 0.33$). This can be related to the well recognized strong metal-support interaction of TiO_2 supported noble metal catalysts, which has been reported extensively in the literature [42–44]. Under reducing conditions at temperatures above 200 °C it has been observed that reduced titania (TiO_x) can migrate onto the surface of the noble metal crystallites thereby strongly modifying or even covering active sites [45,46]. This alters the chemisorption properties of the catalyst, possibly making the adsorption and dissociation of NO a limiting factor for the NH_3 formation. In the presence of oxygen this effect is dampened, which promotes formation of ammonia.

During the WGS-assisted experiments, a clear difference in activity between the Al_2O_3 and SiO_2 supported samples is observed, as compared to the very similar behaviour they exhibit when hydrogen is available in the feed gas. This difference in activity can be due to Al_2O_3 sites that contribute towards rapid hydrolysis of cyanate groups (—NCO) to NH_3 as proposed by Macleod et al. [2] but can also be ascribed to the enhanced H_2 formation ability during the WGS reaction itself over Al_2O_3 compared to SiO_2 as observed in Fig. 3c. It is of importance at this point to state that both cyanate hydrolysis and WGS activity seem to have an influence on the NH_3 formation during this reaction. The increase in concentration of CO_2 observed in Fig. 3b compared to Fig. 3c, as a result of the addition of NO into the gas feed, may be explained by the hydrolysis of the cyanate groups to form NH_3 and CO_2 (Eqs. 5–8). This explains the enhanced NH_3 formation in the temperature range 200–400 °C as compared to the WGS activity of the samples in this region when the stoichiometric requirement of H_2 needed for NH_3 formation (Eq. 3) is not met. The results obtained during the *in situ* DRIFTS experiments over Al_2O_3 also support the proposition of NH_3 being formed by hydrolysis of cyanates since, as previously mentioned, an initial increase in intensity of cyanate vibration followed by a decrease can be observed. The decrease in cyanate intensity is also accompanied by an increase in the intensity of the NH_3 stretching region.

During the steady-state experiments, when the effect of the stoichiometric number on the formation of NH_3 was investigated, 500 ppm O_2 was chosen as the most significant concentration to focus the experiment around since it is the stoichiometric concentration required for complete oxidation of H_2 to H_2O, a factor which was thought to be the limiting factor for the formation of NH_3 in the presence of O_2. It can be seen that NH_3 formation begins when there is insufficient O_2 available for the total oxidation of H_2, suggesting that this is indeed a limiting factor in the production of NH_3 over the catalysts. It is also evident that NH_3 formation is possible at slightly higher oxygen concentrations (S-values) when hydrogen is directly available in the feed as compared to WGS reaction conditions. This may be explained by the fact that, in the case of the WGS reaction, there is more than one reductant that can be oxidized over the catalyst. Due to the presence of CO, it may be even more necessary to limit the presence of O_2 in the system since it has such a strong impeding effect on the production of NH_3. The proposal that the oxidation of CO to CO_2 and hence limitation of H_2 formation as a result of the presence of oxygen in the feed being the main cause of NH_3 suppression seems *via*ble from the DRIFT spectra obtained. This can be said because as the intensity of the CO_2 vibration decreases, a growth in intensity of the NH_3 stretching region is observed. However, since isocyanate hydrolysis is an alternative pathway for the formation of NH_3 which has led to much discussion in this work, the absence of peaks representative of adsorbed —CNO whilst in the presence of excess O_2 should not be ignored. This indicates that an additional explanation for the reduced activity in the presence of excess O_2 is the inhibition of the formation of isocyanate surface species.

5. Conclusions

This study shows that under oxygen deficient conditions it is possible to form significant amounts of NH_3 from nitric oxide and H_2 or water *via* the WGS reaction over silica, alumina and titania supported platinum and palladium in the temperature interval 200–450 °C. However, the formation of ammonia is considerably suppressed in the presence of O_2. The Al_2O_3 supported Pd stands out as a promising material for passive SCR applications not only because it is active over a broad temperature range when H_2 is directly available in the gas feed, but also due to high activity for the WGS assisted reaction, exhibiting a lower light-off temperature than its Pt-containing counterpart.

In situ DRIFT spectroscopy experiments support that when water is used as the source of hydrogen, there is more than one reaction route possible for NH_3 formation; direct reaction of H_2 with stored NO but also hydrolysis of cyanate groups. It also shows that both the inhibition of the water–gas-shift reaction and the suppression of isocyanate surface species due to the presence of oxygen in the feed may be responsible for NH_3 suppression over the investigated catalysts.

Concerning the TiO_2 samples in this investigation, these need to be thermally stabilised in order to be suitable for use in automotive applications as it seems that the formation of large TiO_2 particles leads to low activity. Stabilisation would also be necessary in order to successfully characterise the mechanisms behind NH_3 formation at high temperature.

Acknowledgments

This work was financially supported by the Swedish Energy Administration through the FFI program and the Competence Centre for Catalysis, which is financially supported by Chalmers University of Technology, the Swedish Energy Agency and the member companies: AB Volvo, ECAPS AB, Haldor Topsøe A/S, Volvo Car Corporation, Scania CV AB, and Wärtsilä Finland Oy.

References

[1] M.A. Gómez-García, V. Pitchon, A. Kiennemann, Environ. Int. 31 (2005) 445–467.
[2] N. Macleod, R. Cropley, J.M. Keel, R.M. Lambert, J. Catal. 221 (2004) 20–31.
[3] Y. Liu, M.P. Harold, D. Luss, Appl. Catal. B: Environ. 121 (2012) 239–251.
[4] S.M. Park, M.-Y. Kim, E.S. Kim, H.-S. Han, G. Seo, Appl. Catal. A: Gen. 395 (2011) 120–128.
[5] A. Lindholm, N. Currier, J. Li, A. Yezerets, L. Olsson, J. Catal. 258 (2008) 273–288.
[6] N. Macleod, R.M. Lambert, Appl. Catal. B: Environ. 46 (2003) 483–495.
[7] C. Ciardelli, I. Nova, E. Tronconi, D. Chatterdee, T. Burkhardt, M. Weibel, Chem. Eng. Sci. 62 (2007) 5001–5006.
[8] P. Forzatti, L. Lietti, I. Nova, E. Tronconi, Catal. Today 151 (2010) 202–211.
[9] M. Koebel, M. Elsener, M. Kleemann, Catal. Today 59 (2000) 335–345.
[10] G. Li, C. Jones, V. Grassian, S. Larsen, J. Catal. 234 (2005) 401–413.
[11] P.R. Dasari, R. Muncrief, M.P. Harold, Catal. Today 184 (2012) 43–53.
[12] N.V. Heeb, A.-M. Forss, S. Brühlmann, R. Lüscher, C.J. Saxer, P. Hug, Atmos. Environ. 40 (2006) 5986–5997.
[13] T.D. Durbin, J.T. Pisano, T. Younglove, C.G. Sauer, S.H. Rhee, T. Huai, J.W. Miller, G.I. MacKay, A.M. Hochhauser, M.C. Ingham, R.A. Gorse, L.K. Beard, D. DiCicco, N. Thompson, R.J. Stradling, J.A. Rutherford, J.P. Uihlein, Atmos. Environ. 38 (2004) 2699–2708.
[14] C.D. DiGulio, J.A. Pihl, J.E. Parks II, M.D. Amiridis, T.J. Toops, Catal. Today 231 (2014) 33–45.
[15] F. Can, X. Courtois, S. Royer, G. Blanchard, S. Rousseau, D. Duprez, Catal. Today 197 (2012) 144–154.
[16] R.D. Clayton, M.P. Harold, V. Balakotaiah, Appl. Catal. B: Environ. 81 (2008) 161–181.
[17] N.W. Cant, D.C. Chambers, I.O.Y. Liu, Appl. Catal. B: Environ. 46 (2003) 551–559.
[18] M.L. Unland, Science 179 (1973) 567–569.
[19] S. Brunauer, P.H. Emmett, E. Teller, J. Am. Chem. Soc. 60 (1938) 309–319.
[20] H. Kannisto, X. Karatzas, J. Edvardsson, L.J. Pettersson, H.H. Ingelston, Appl. Catal. B: Environ. 104 (2011) 74–83.

[21] J.C. Summers, K. Baron, J. Catal. 57 (1979) 380–389.
[22] S.K. Matam, E.V. Kondratenko, M.H. Aguirre, P. Hug, D. Rentsch, A. Winkler, A. Weidenkaff, D. Ferri, Appl. Catal. B: Environ. 129 (2013) 214–224.
[23] C.R. Bickmore, K.F. Waldner, R. Baranwal, T. Hinklin, D.R. Treadwell, R.M. Lain, J. Eur. Ceram. Soc. 18 (1998) 287–297.
[24] H.A. Benesi, A.C. Jones, J. Phys. Chem. 63 (1959) 179–182.
[25] S. Yamazoe, T. Okumura, Y. Hitomi, T. Shishido, T. Tanaka, J. Phys. Chem. 111 (2007) 11077–11085.
[26] S.M. Lee, S.C. Hong, Appl. Catal. B: Environ. 163 (2015) 30–39.
[27] C. Morterra, G. Magnacca, Catal. Today 27 (1996) 497–532.
[28] T.J. Toops, D.B. Smith, W.S. Epling, J.E. Parks, W.P. Partridge, Appl. Catal. B: Environ. 58 (2005) 255–264.
[29] S.-H. Chien, M.-C. Kuo, C.-H. Lu, K.-N. Lu, Catal. Today 97 (2004) 121–127.
[30] D.D. Miller, S.S.C. Chuang, J. Taiwan Inst. Chem. Eng. 40 (2009) 613–621.
[31] S. Almusaiteer, S.S.C. Chuang, J. Catal. 201 (1999) 189–201.
[32] I. Nova, L. Lietti, P. Forzatti, F. Prinetto, G. Ghiotti, Catal. Today 151 (2010) 330–337.
[33] C. Neyertz, D. Volpe, D. Perez, I. Costilla, M. Sanchez, C. Gigola, Appl. Catal. A: Gen. 368 (2009) 146–157.
[34] Y. Ji, T.J. Toops, J.A. Pihl, M. Crocker, Appl. Catal. B: Environ. 91 (2009) 329–338.
[35] T. Nanba, F. Meunier, C. Hardacre, J.P. Breen, R. Burch, S. Masukawa, J. Uchisawa, A. Obuchi, J. Phys. Chem. C. 112 (2008) 18157–18163.
[36] L. Castoldi, R. Bonzi, L. Lietti, P. Forzatti, S. Morandi, G. Ghiotti, S. Dzwigaj, J. Catal. 282 (2011) 128–144.
[37] J. Choi, W.P. Partridge, J.A. Pihl, M.-Y. Kim, P. Koci, C.S. Daw, Catal. Today 184 (2012) 20–26.
[38] A. Vazquez-Zavala, J. García-Gómez, A. Gómez-Cortés, Appl. Surf. Sci. 167 (2000) 177–183.
[39] A. Priebe, G. Fahsold, A. Pucci, J. Phys. Chem. 108 (2004) 18174–18178.
[40] N.W. Cant, D.C. Chambers, I.O.Y. Liu, J. Catal. 231 (2005) 201–212.
[41] N. Macleod, R.M. Lambert, Appl. Catal. B: Environ. 35 (2002) 269–279.
[42] J.C. Colmenares, A. Magdziarz, M.A. Aramendia, A. Marinas, J.M. Marinas, F.J. Urbano, J.A. Navio, Catal. Commun. 16 (2011) 1–6.
[43] M.S. Spencer, J. Catal. 93 (1985) 216–223.
[44] O. Dulub, W. Habenstreit, U. Diebold, Phys. Rev. Lett. 84 (2000) 3646–3649.
[45] S. Jacinto, J. Bernardi, J.A. Anderson, Catal. Lett. 114 (2007) 91–95.
[46] F. Pesty, H.P. Steinruck, T.E. Madey, Surf. Sci. 339 (1995) 83–95.